BOLETIN DE LA SOCIEDAD ESPAÑOLA DE
Cerámica y Vidrio
A R T I C U L O

Effect of a CGO buffer layer on the performance of $(La_{0.6}Sr_{0.4})_{0.995}Co_{0.2}Fe_{0.8}O_{3-\delta}$ cathode in YSZ-Based SOFC

J. PEÑA-MARTÍNEZ[1,2], D. MARRERO-LÓPEZ[3], C. SÁNCHEZ-BAUTISTA[1], A.J. DOS SANTOS-GARCÍA[1], J.C. RUIZ-MORALES[2], J. CANALES-VAZQUEZ[1], P. NÚÑEZ[2]

[1]Instituto de Investigación en Energías Renovables, Universidad de Castilla La Mancha, Parque Científico y Tecnológico de Albacete, 02006-Albacete, Spain
[2]Departamento de Química Inorgánica, Universidad de La Laguna, 38200-Tenerife, Spain
[3]Departamento de Física Aplicada I, Universidad de Málaga, 29071-Málaga, Spain

The electrochemical properties of $(La_{0.6}Sr_{0.4})_{0.995}Co_{0.2}Fe_{0.8}O_{3-\delta}$ (LSCF) and LSCF-gadolinium-doped ceria (CGO) composite electrodes towards oxygen reduction were studied by impedance spectroscopy in a symmetric cell configuration using yttria-stabilised zirconia (YSZ) as electrolyte and a CGO buffer layer between the electrode and the electrolyte materials. The best polarisation resistance values were obtained for a LSCF-CGO (60/40, wt.%) composite with values ranging between 0.07 and 0.4 Ωcm^2 in the temperature range of 650-775ºC. The effect of the CGO buffer on the polarisation resistance of the LSCF electrode and the series resistance of the symmetrical LSCF/YSZ cell was also investigated. In addition, X-ray diffraction analysis was carried out to study the chemical compatibility between LSCF, YSZ and CGO materials.

Keywords: CGO-buffer layer, Cathode, LSCF, MIEC, Polarisation resistance, SOFC

Efecto de una capa intermedia de CGO en el Rendimiento de $(La_{0.6}Sr_{0.4})_{0.995}Co_{0.2}Fe_{0.8}O_{3-s}$ como cátodo en pilas SOFC con YSZ

Las propiedades electroquímicas de los electrodos $(La_{0.6}Sr_{0.4})_{0.995}Co_{0.2}Fe_{0.8}O_{3-\delta}$ (LSCF) y composites de LSCF con ceria dopada con gadolinio (CGO), respecto la reacción de reducción del oxígeno, fueron estudiadas mediante espectroscopía de impedancia usando una configuración de celda simétrica, con circonia estabilizada con itria (YSZ) como electrolito y CGO como capa de protección entre el material de electrodo y electrolito. Los mejores valores de resistencia de polarización fueron obtenidos para el composite LSCF-CGO (60/40, % en peso) con valores comprendidos entre 0,07 y 0,4 Ωcm^2 para el rango de temperaturas de 650-775ºC. El efecto de la capa intermedia de CGO sobre la resistencia de polarización del electrodo LSCF y la resistencia en serie de la celda simétrica LSCF/YSZ fue también investigado. La compatibilidad química de LSCF, YSZ y CGO se ha estudiado mediante difracción de rayos X.

Palabras clave: Capa intermedia de CGO, Cátodo, LSCF, MIEC, Resistencia de polarización, SOFC

1. INTRODUCTION

Solid oxide fuel cells (SOFCs) are electrochemical power generation devices characterised by high-energy conversion efficiency, low pollution and fuel flexibility (1). However, typical SOFCs operate at 1000ºC, and the elevated temperature introduces a series of problems such as sintering of the electrodes and high reactivity between the cell components. For these reasons, there is a considerable research interest in reducing the operating temperature of SOFCs in the range from 500 to 800°C because this would imply the use of inexpensive metallic materials, rapid start-up and shut-down, minimisation of thermal degradation and reactions between the cell components (2). However, resistive losses across the solid electrolyte and electrode overpotentials increase with the drop of the operation temperature. Different approaches to minimize resistive losses across the electrolyte have been adopted such as replacing the state-of-the-art yttria-stabilized zirconia (YSZ) by alternative solid electrolytes e.g. doped-ceria with higher ionic conductivity, and using thinner solid electrolytes. The vast majority of the thin film SOFCs use YSZ as electrolyte, because YSZ is characterised by good chemical and mechanical stability with high quality raw materials available (3,4). Assuming that the electrolyte should not contribute more than 0.15 Ωcm^2 to the total cell area-specific resistance (5), in thin film form, the thickness of the YSZ-film should be 10-15 μm in order to operate at 700ºC. YSZ film of 10-15 μm can be reliably mass-produced using relatively cheap ceramic fabrication routes. Therefore, it seems reasonable to study the YSZ-based systems for applications at 700ºC. Otherwise, it is unlikely that YSZ-based systems will operate below 700ºC because the intrinsic resistance of the material becomes too high. For lower temperatures, alternative electrolytes with higher oxygen ion conductivity can be considered as aforementioned e.g. doped lanthanum gallate or doped-ceria materials, although these might introduce new difficulties such as higher reactivity, electronic conductivity, or thermal expansion mismatch (3).

On the other hand, one of the major problems of decreasing the operation temperature, apart from the enhanced ohmic

losses at the electrolyte, is the increase of the cathodic overpotential. Hence, new cathode materials with low polarisation resistance must be developed (6). The mixed ionic electronic conductors (MIECs) based upon $LaCoO_3$, particularly those substituted with Sr and Fe on La and Co sites respectively, i.e. $La_{1-x}Sr_xCo_{1-y}Fe_yO_{3-\delta}$, have attracted great interest due to their high catalytic activity towards the oxygen reduction, high electrical conductivity and superior surface oxygen exchange and bulk diffusion compared to those of conventional Sr-doped $LaMnO_3$ cathodes (7-15). The properties of these cobalt-ferrites depend on their composition, namely the combination of x and y (16,17). $La_{0.6}Sr_{0.4}Co_{0.2}Fe_{0.8}O_{3-\delta}$ (LSCF) is usually the preferred composition for a good compromise between conductivity, catalytic activity, thermal expansion coefficient (TEC) and reactivity with the electrolyte (8). Nevertheless, area-specific resistance values from 0.07 to 0.7 Ωcm^2 for pure LSCF or LSCF-CGO composite have been reported by different authors using YSZ as electrolyte at 700ºC (11). Wang and Mogensen (8) reported polarisation resistance values of 0.6 Ωcm^2 at 600ºC and 0.12 Ωcm^2 at 700ºC on YSZ electrolyte coated with a thinner layer of CGO. Furthermore, these authors found a similar value on YSZ electrolyte directly without a buffer layer, i.e. 0.13 Ωcm^2 at 700ºC. In fact, they concluded that the LSCF cathode may be used directly on the YSZ electrolyte without CGO coating, although in this case the operation temperature must be below 800ºC according to an ageing study of the LSCF-CGO composite cathode on YSZ electrolyte. The results showed modest increase of the polarisation resistance and no obvious increase of the serial resistance after 180 h of operation at 800ºC. The aim of this work is to investigate further the polarisation resistance of LSCF on YSZ with and without a CGO-buffer layer, including a 360 h test at 700ºC.

2. EXPERIMENTAL PROCEDURE

Commercial powders of $(La_{0.6}Sr_{0.4})_{0.995}Co_{0.2}Fe_{0.8}O_3$ (LSCF), 8 mol% Y_2O_3 in ZrO_2 (YSZ) and $Ce_{0.8}Gd_{0.2}O_{2-\delta}$ (CGO) supplied by Fuel Cell Materials, Pi-KEM and Praxair respectively, have been used to prepare the symmetric electrode cells with dense YSZ electrolytes (98-99% of theoretical density) as described in Ref. 18. The surface area of the LSCF starting powders was 6.1 m^2g^{-1}, whereas two different CGO powders were used to prepare various LSCF-CGO composites, one characterised by a low surface area, i.e. 4 m^2g^{-1} (CGO-4) and the second with high surface area, i.e. 200 m^2g^{-1} (CGO-200). Slurries of the LSCF, CGO and LSCF-CGO composites (10, 25, 40 and 50 wt.% of CGO) were prepared using Decoflux™ as organic vehicle. CGO-4 (low surface area) buffer layers were coated on both surfaces of the YSZ dense pellets and fired at 1100-1300ºC for 2 h. It should be mentioned that using CGO-200 (high surface area) to prepare a buffer layer implied a firing temperature above 1200ºC in order to ensure an adequate adherence, consequently the use CGO-200 to fabricate the buffer layer was discarded and was only used to prepare LSCF-CGO composites. Therefore, when CGO buffer layer is mentioned, this is comprised of CGO-4.

A thin layer of the LSCF slurry was coated directly on both sides of the electrolyte or on the CGO buffer layers, with 0.24 cm^2 of electrode area, and then fired at 800-1000ºC for 2 hours in air. The thickness of the electrode layer after firing was in every case about 20-30 μm. Porosity, adherence and microstructure of the deposited electrodes were studied by scanning electron microscopy (SEM) (JEOL JSM-6300) revealing an average porosity of ~30%. The current collector was formed by coating platinum paste on both sides of the pellets and then fired at 800ºC for 1 h. Another electrodes were prepared using the different LSCF-CGO-composites slurries on the CGO buffer layers and fired at 900ºC for 2 h, which was the appropriate temperature, taking into account the lower polarisation resistance of the LSCF/CGO/YSZ system fired at different temperatures i.e. 825-1000ºC (explained in the Results and Discussion section).

The overall conductivity of LSCF and the area-specific resistance (polarisation resistance) of the electrode materials was measured by the Van der Pauw method and electrochemical impedance spectroscopy respectively as described in Ref. 19 and 20. The ASR was determined from the impedance spectra, where the highest frequency intercept is due primarily to the electrolyte resistance usually named serial resistance (R_s), while the difference between the high and low frequency intercepts on the real axis (Z´) is associated to the electrode contribution.

X-Ray diffraction analysis (Panalytical X´Pert Pro diffractometer equipped with a primary monochromator, $CuK\alpha_1$ radiation, and the X´Celerator detector) was also carried out to investigate the crystal structure and chemical compatibility of LSCF with YSZ and CGO oxides. Regarding reactivity, powder mixtures of LSCF with the corresponding oxide, YSZ or CGO, in a 1:1 ratio (wt.%), were ground in an agate mortar and fired at 700, 900 and 1200ºC for 10-20 h in air, cooled down to room temperature and studied by XRD. Chemical compatibility between the YSZ electrolyte and the CGO-buffer material was also studied following the same procedure. In this case, the YSZ-CGO mixture was fired at 700-1400ºC for 10 h. The XRD patterns were collected with a 0.016º step in the 2θ angular range 15-120º and acquisition time of 3 h. Profile matching of the XRD patterns was performed using FullProf and WinPlotr programs (21). Phase identification was performed with X'Pert HighScore Plus v.2.0a software using the ICSD database (22, 23).

3. RESULTS AND DISCUSSIONS

3.1. X-ray diffraction analysis

The XRD pattern for $(La_{0.6}Sr_{0.4})_{0.995}Co_{0.2}Fe_{0.8}O_{3-\delta}$ powders sintered at 900ºC, shown in Fig. 1, was refined in a rhombohedral crystal symmetry, space group $R\bar{3}c$ with cell parameters a= 5.4916(2) Å and c= 13.3683(6) Å, which is in agreement with the literature data (24-26).

Regarding the chemical compatibility between LSCF oxide and YSZ and CGO, XRD patterns at room temperature, 700, 900 and 1200ºC of the binary-mixed-systems LSCF-YSZ and LSCF-CGO are shown in Fig. 2a and 2b respectively. Additional diffraction peaks assigned to $SrZrO_3$ phase were found after firing the LSCF-YSZ mixture at 900ºC (Fig. 2a) indicating a reaction between LSCF and YSZ which is stronger as the temperature increases. Indeed, after firing at 1200ºC some new diffraction peaks, which may be ascribed to $CoFe_2O_4$, $LaFeO_3$ and $SrCoLaO_4$, were identified. The high reactivity of LSCF with YSZ could influence negatively in the

performances of the YSZ-based cells due to the need of high temperatures to fix the electrode material to the electrolyte with an adequate adherence. On the contrary, no additional diffraction peaks can be observed in the LSCF-CGO system after firing the mixture at 900ºC for 10 h, Fig. 2b, revealing that LSCF cathode has a good chemical compatibility with the CGO material, although the diffraction peaks for LSCF at 1200ºC are shifted towards higher angles compared to the origin position at 900ºC, and this seems to indicate cation interdifussion between both materials. Consequently, an optimisation of the firing temperature for fixing the LSCF material on the CGO buffer layer was envisaged, and the results will be discussed in the next section. On the chemical compatibility between CGO and YSZ, see Fig. 2c, a CGO-YSZ solid solution starts to be formed at 1200ºC giving rise to a single phase at 1400ºC, thereby an appropriate firing temperature should be also chosen to fix the CGO buffer on the YSZ electrolyte as (Zr,Ce) O_2-based solutions exhibit much lower ionic conductivities than CGO and YSZ and this may affect the performance of the cell (27).

Another issue to be considered is the mechanical compatibility. The reported TEC value of LSCF at high temperature is over 15×10^{-6} K^{-1} (26), which is higher than that of YSZ, i.e. 10×10^{-6} K^{-1} though closer to CGO, 12.5×10^{-6} K^{-1}. Therefore, the use of a CGO buffer layer and LSCF-CGO composites may be regarded as a practical solution to avoid mechanical and chemical mismatches between LSCF and YSZ.

3.2. Overall conductivity

The overall electrical conductivity of LSCF in air as a function of the temperature is represented in Fig. 3. The values of conductivity are similar to those reported in the literature (17,26). The conductivity initially increases with the temperature up to 600ºC. At higher temperatures the conductivity decreases due to the loss of lattice oxygen as consequence of the partial reduction of the Fe and Co ions from higher to lower

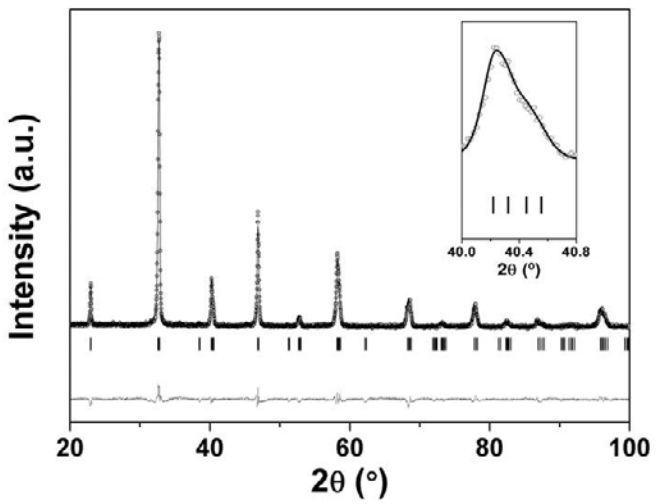

Fig. 1. XRD pattern of LSCF analysed by the Rietveld method after calcination at 900ºC for 2 h in air. The open circles are the observed intensity, the black line is the calculated intensity; below is the difference plot between the observed and calculated intensities.

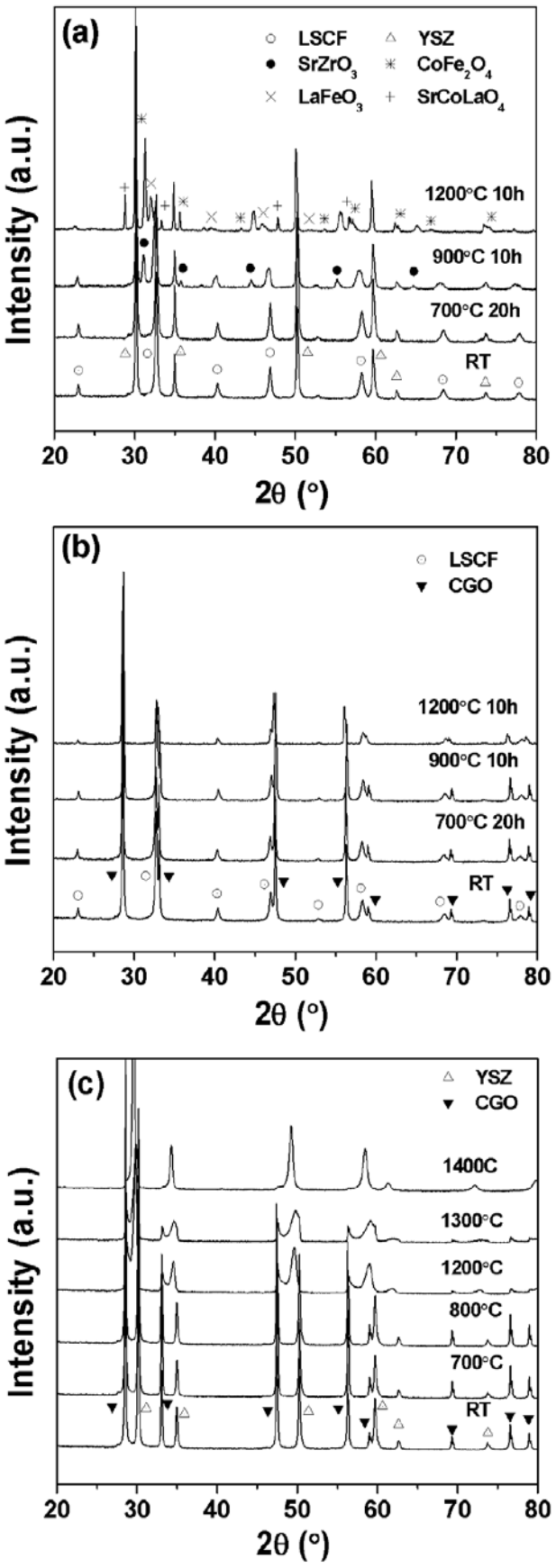

Fig. 2. XRD Patterns for LSCF/YSZ (a), LSCF/CGO (b) and YSZ/CGO (c) mixtures (1:1 wt.%), at room temperature (RT) and fired at 700-1400ºC for 10-20 h in air. Diffraction peaks for LSCF, YSZ and CGO phases and reaction products are indicated in the figure.

oxidation states. The negative temperature dependence of the conductivity above 600ºC is due to a decrease in the *p*-type electronic carriers via formation of oxygen vacancies (16,17,24,25). The observed electrical conductivity drop is significant, although the total conductivity remains above 200 Scm^{-1} in the whole temperature range (300-900ºC).

3.3. Area-specific resistance and impedance analysis

Symmetrical cells using pure LSCF and LSCF-CGO composites were prepared in order to measure their ASR value in air. First of all, it was investigated the appropriate temperature for fixing the CGO layer on the YSZ electrolyte and afterwards the LSCF on the CGO-buffer layer. Hence, Fig. 4a shows the ASR values of the CGO/YSZ symmetrical cells. The YSZ pellet coated with CGO layers sintered at 1200ºC presented the lowest ASR and serial resistance values (Fig. 4a and 4b). Taking into account the reactivity between CGO and YSZ, see section 3.1, the CGO layer fired at 1200ºC exhibited an adequate particle distribution and adherence as can be observed in the SEM images (Fig. 5). Therefore, the higher polarisation and serial resistance of the CGO/YSZ samples sintered at 1100 and 1300ºC is related possibly to a loss of adherence and high reactivity respectively. It is worth noting that certain degree of reactivity between CGO and YSZ was also found at 1200ºC for 10h, which is stronger at 1300ºC as shown in Fig. 5b, therefore some interfacial reaction may be expected in long-term operations. For instance, Fue *et al.* (10) sintered a samarium doped ceria interlayer on YSZ electrolyte at 1300ºC for 8 h. These high temperature and long dwell time might be the main reason for the high polarisation resistance values reported (0.55 Ωcm^2 at 700ºC) of the studied LSCF-SDC composite cathode. However, Wang and Mogensen (8) sintered a CGO-buffer layer on YSZ at the same temperature (1300ºC) and reported a polarisation resistance for a LSCF-CGO composite cathode as low as 0.12-0.14 Ωcm^2 at 700ºC.

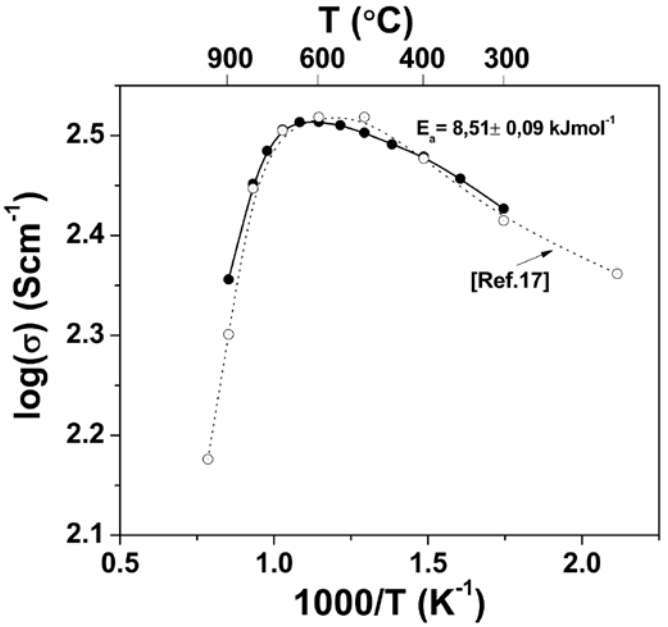

Fig. 3. Electrical conductivity of $(La_{0.6}Sr_{0.4})_{0.995}Co_{0.2}Fe_{0.8}O_{3-\delta}$ measured during cooling in air. Conductivity values from reference (17) are included for comparison.

Further investigation is now in progress in order to optimise the deposition of the buffer layer at lower temperature.

Considering the optimum temperature for fixing pure LSCF on YSZ with a CGO-buffer layer, the ASR values measured at 700ºC in air of the symmetrical cells, LSCF/CGO/YSZ, with LSCF sintered at different temperatures, are represented in Fig. 6. As can be observed, the sample with LSCF fired at 900ºC for 2 h presented the lowest ASR value, 0.325 Ωcm^2 at 700ºC. As a result, the LSCF-CGO composites were fixed on YSZ with a CGO buffer layer at 900ºC for 2h. Without a buffer

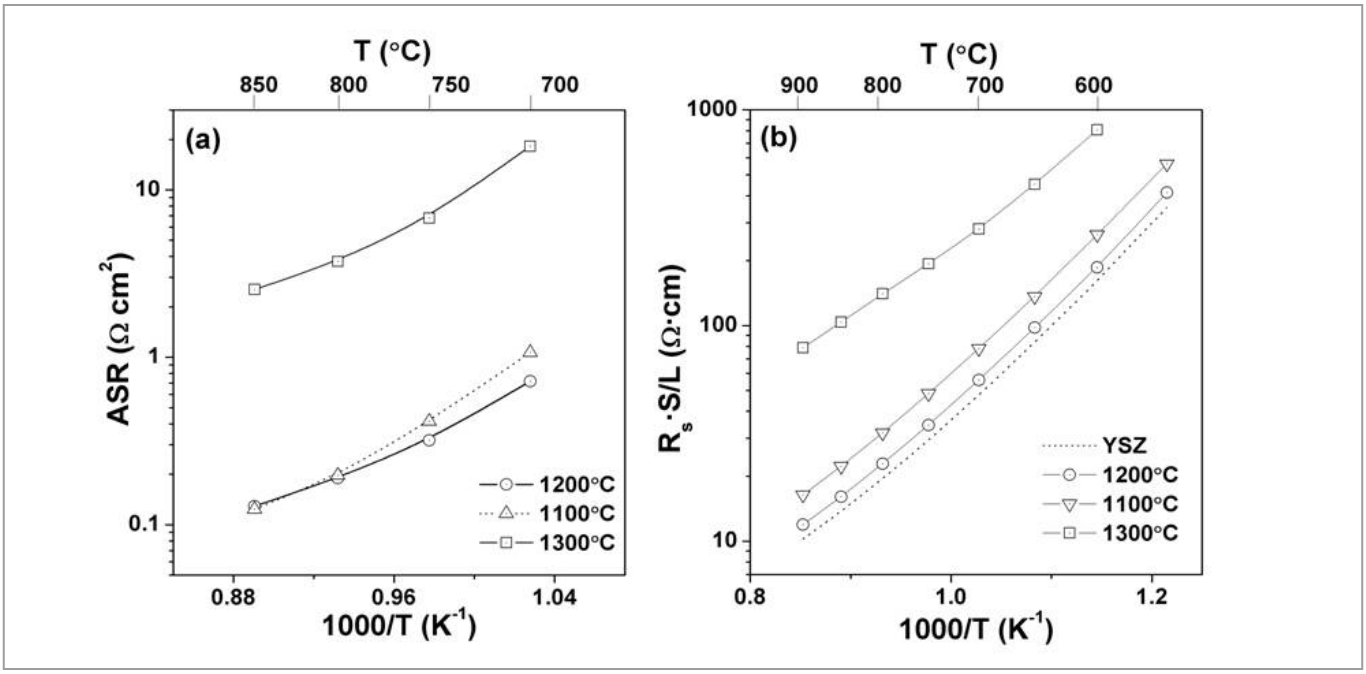

Fig. 4. (a) Area-specific resistance (ASR) and (b) serial resistance (R_s) normalised by the thickness (L) and electrode-area (S) of the CGO/YSZ symmetrical cells. R_s values from symmetrical Platinum/YSZ cells (dash line) are included in (b) for comparison.

layer, the best temperature in order to fix LSCF on YSZ is 800ºC for 2 h, taking into account the corresponding ASR values of the symmetrical LSCF/YSZ cell i.e. 0.5 Ωcm² at 700ºC. These values are rather high for practical applications and higher than those of the LSCF/YSZ symmetrical cell with a CGO-buffer layer (0.325 Ωcm² at 700ºC). Such poor performance might be due to a poor adherence and/or segregation of secondary phases as aforementioned in the chemical compatibility study. Moreover, after 360 h of operation at 700ºC, the ASR values of the system with and without a CGO-buffer layer between pure LSCF and YSZ increase up to 0.86 Ωcm² and 2.0 Ωcm² respectively, see Fig. 7. In addition, the serial resistance (R_s) increases though the effect is not as significant as in the case of the polarisation resistance i.e. from 4.15 to 4.46 Ωcm² (7%) for the LSCF/YSZ system and from 4.85 to 4.99 Ωcm² (3%) for the buffered system. This is in good agreement with the results found by Wang and Mogensen (8). One may observe that the R_s for the CGO coated YSZ electrolyte compared to that for uncoated YSZ is slightly higher and this is due to an extra contribution from the CGO layer. Anyway, it is clear that without the buffer layer the polarisation resistance is higher and according to the previous results of chemical compatibility, the reactivity between LSCF and YSZ may lead to a detrimental interfacial reaction giving rise to an increase of the polarisation resistance, hence an increase of the cathodic overpotential. On the other hand, the increase of R_s is not as large as to indicate poor adhesion between the cell components or an obvious reaction between them. Wang and Mogensen (8) suggested a process of densification of the LSCF material rather than a reaction between LSCF and YSZ although they did not find any evidence for that claim by SEM. In the present case, SEM image of the cross section of the LSCF/YSZ interface after the 360 h of operation at 700ºC is illustrated in Fig. 8 and as pointed out in Ref. 8 no sign of particle sintering was found.

The impedance spectra were conveniently analysed in order to identify a possible degradation process which could be attributed to the observed increase in the polarisation resistance with time (Fig. 9a and 9b). The data were also corrected considering the electrode area and divided by 2, given the use of symmetrical cells (20). From a qualitative point of view two major contributions were observed in the impedance spectra. In order to separate the different contributions, the impedance spectra were fitted by the ZView software (28) using equivalent circuits (inset of Figure 9a and 9b) as described in Ref. 19 and 20 i.e. $LR_s(RQ)_{HF}(RQ)_{LF}$ where L represents the inductance of the equipment, R_s is a serial resistance associated to the overall cell resistance, and two serial RQ-elements associated to the electrode processes where R is a resistance and Q is a constant phase element in parallel. The subscripts HF and LF refer to the high and low frequency arcs respectively. It should be noted that in case of the symmetrical systems without buffer layer a better fit of the spectra was obtained using a Warburg or diffusion circuit element instead of the first (RQ) element, suggesting the idea that some diffusion processes occurs in the LSCF/YSZ interface, and this agrees with the high reactivity found between LSCF and YSZ. Regarding the increase of the resistance value of the (RQ) elements, see Fig. 10, one can conclude that both processes at high and low frequency dominate the detrimental increase of the overall polarisation resistance in the case of the system without buffer, whereas the low-frequency process dominates

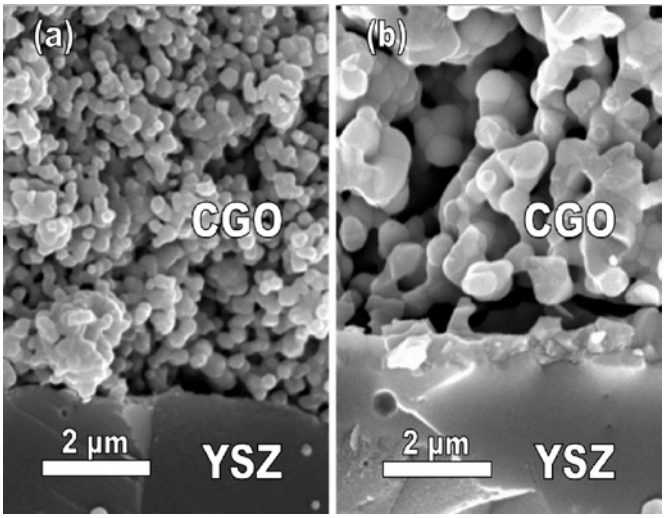

Fig. 5. SEM images of the CGO/YSZ interface of the CGO/YSZ symmetrical cells fired at 1200ºC (a) and 1300ºC (b) for 2 h.

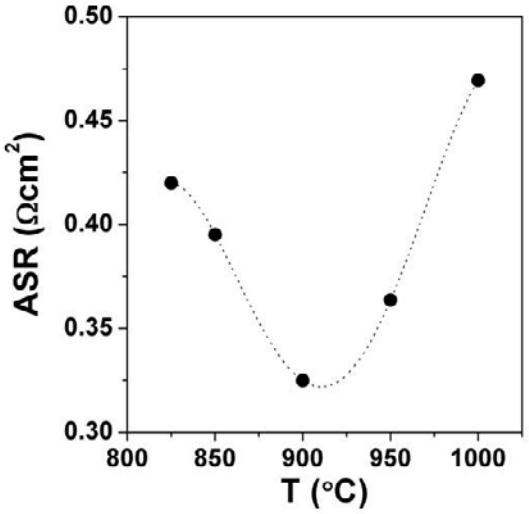

Fig. 6. Area-specific resistance (ASR) measured at 700ºC in air for the LSCF/CGO/YSZ system as a function of the fixing temperature for the LSCF layers.

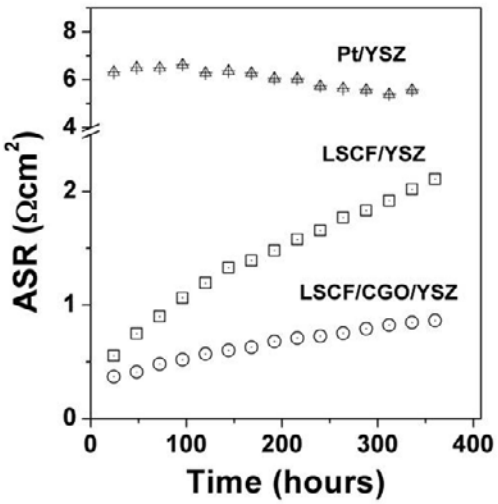

Fig. 7. Area-specific resistance (ASR) for the LSCF/YSZ and LSCF/CGO/YSZ systems at 700ºC as a function of operation time. ASR values of Platinum electrode coated on YSZ at 700ºC are included for comparison.

the increase of the polarisation resistance when the CGO-buffer layer is used. Furthermore, for the system with buffer, the n-values for Q_{LF} vary between 0.76 and 0.79 suggesting that Q is mainly a capacitive element, whereas for Q_{HF}, the n-value ranges from 0.46 to 0.53. As this value is near 0.5 the process might reflect surface and/or bulk diffusion limitations. Without the CGO-buffer layer, the n-values for Q_{LF} vary also between 0.76 and 0.81, whilst the use of a Warburg element for the high frequency process indicates some diffusion limitation as well as in the former buffered system. In order to know more about the processes involved in the system with buffer, the capacitive elements of the equivalent circuit fitting were investigated in greater detail. Due to depressed semicircles, constant phase elements, Q, were used in the fitting procedure, and these pseudo-capacitive elements were transformed into comparable capacitances as described in Ref. 20.

The corresponding capacitive elements and relaxation frequencies were on the order of 10^{-4} Fcm^2 and 1 kHz for the low frequency process and 10^{-6} Fcm^2 and 1 MHz for the high frequency contribution (Fig. 11). This indicates that these arcs correspond to electron and oxide-ion charge-transfer processes respectively (9,29). Therefore, the electron charge-transfer process may be limited as the time of operation increases. In this context, Fu *et al.* (10) reported that the oxygen reduction reaction on a porous LSCF-samarium doped ceria electrode was limited primarily by the charge transfer process, presumably occurring at the triple phase boundary and this agrees with our results. These authors also suggested that improving the interface contact and expanding the TPB accelerates the rate of oxygen reduction on the LSCF-doped ceria composite. On the other hand, Yokokawa *et al.* (30) investigated the potential diffusion of Sr through the ceria-based interlayer between (La,Sr)MO_3 (M=Fe,Co) and YSZ, which might lead to the formation of $SrZrO_3$ at the interface between ceria and YSZ, which in turn would affect the charge transfer processes. They reported that the stability of the three-layer structure cathode/doped-ceria/YSZ electrolyte is affected strongly by

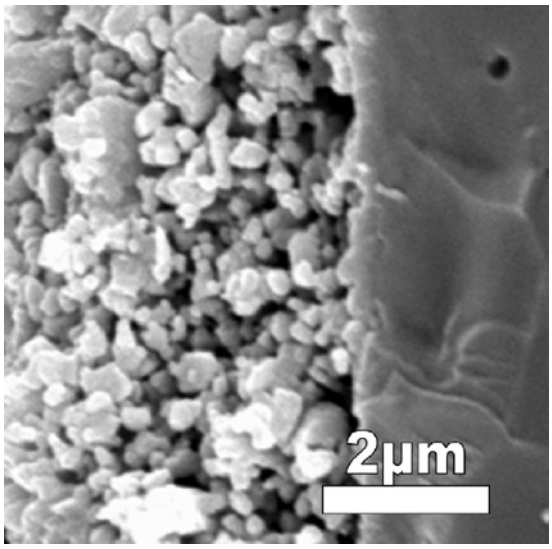

Fig. 8. SEM images of the LSCF/YSZ interfaces after 360 h of operation at 700ºC.

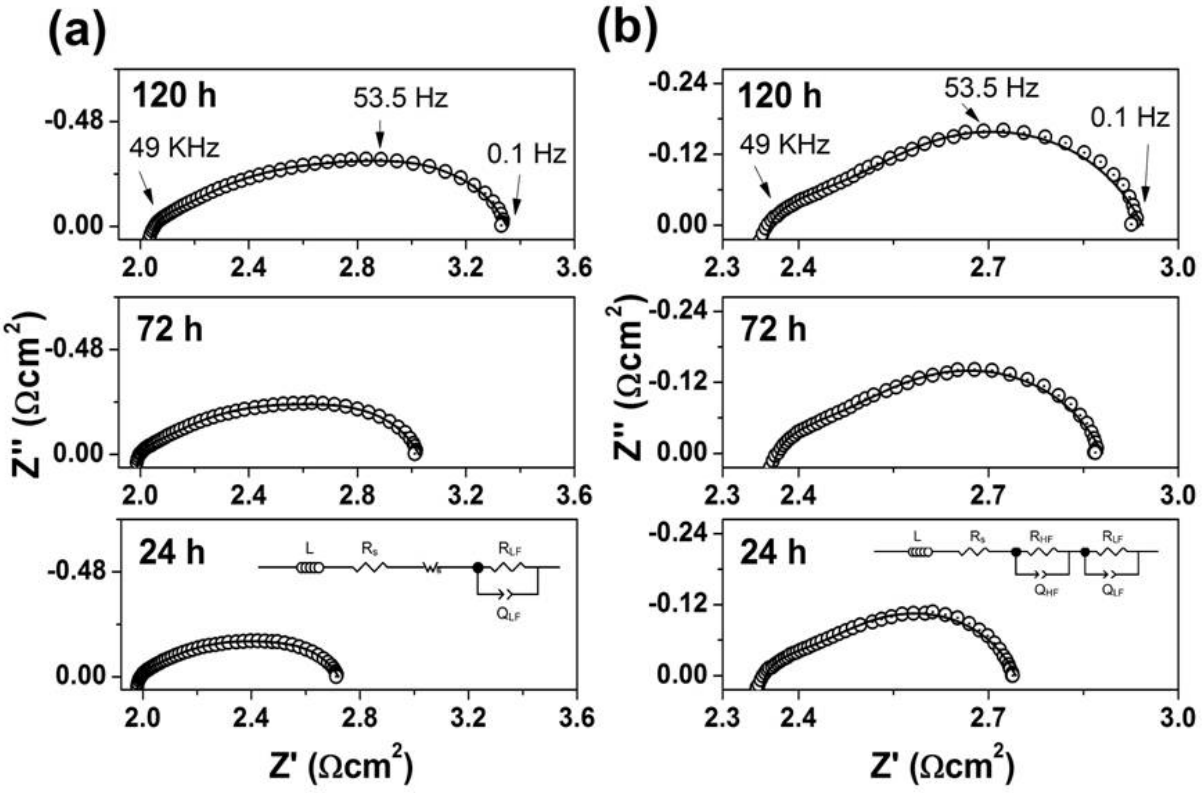

Fig. 9. Impedance spectra for LSCF/YSZ (a) and LSCF/CGO/YSZ (b) after 24, 72 and 120 h during ageing test at 700ºC in air. The insets show the equivalent circuits used to fit the spectra. The solid line is the fitting result using equivalent circuits.

the oxidation state of iron and cobalt oxides, and the driving force for the formation of $SrZrO_3$ depends on the chemical potential of SrO at the cathode/doped ceria interfaces. In the present case, there is no clear evidence for the formation of $SrZrO_3$ at the CGO/YSZ interface, which would be rather difficult if one considers that our CGO-buffer layer is a 10-μm thick interlayer. Nevertheless, further investigation is in progress to clarify this point.

On the other hand, the ASR value of 0.325 Ωcm^2 at 700ºC obtained for the LSCF/CGO/YSZ system is rather high if one considers a target value of 0.15 Ωcm^2 (5). One approach to decrease cathode polarisation is the addition of an ionic conducting phase, CGO in the present case, to obtain a composite. The temperature dependence of the ASR for the LSCF-CGO composites measured over a temperature range of 650-775ºC in air is presented in Fig. 12. The symmetric cell using LSCF-CGO with 40 wt.% CGO-4 (low surface area) showed the lowest ASR values in the temperature range studied, e.g. 0.2 Ωcm^2 at 700ºC (E_a=117±2 kJmol^{-1}), which is slightly higher than the value of 0.12-0.14 Ωcm^2 at 700ºC (E_a=116 kJmol^{-1}) reported by Wang *et al.* (8) for LSCF-CGO samples with 50 wt.% CGO, but lower than those reported by Fu *et al.* (10) i.e. 0.55 Ωcm^2 at 700ºC (E_a=282 kJmol^{-1}) for LSCF-$Ce_{0.8}Sm_{0.2}O_{2-\delta}$ composite with 50 wt.% LSCF, and comparable to those reported by Esquirol *et al.* (7), i.e. 0.2-0.4 Ωcm^2 at 650ºC (Ea=131 kJmol^{-1}) for the system LSCF-CGO (30 wt.% CGO) on CGO.

In summary, LSCF-CGO composites are good candidates as cathode material for intermediate temperature SOFCs using YSZ as electrolyte and a CGO interlayer. Nevertheless, this buffer layer must be optimised and long term operation tests should be carried out to elucidate the stability of the electrochemical response in the LSCF-CGO/CGO/YSZ system.

4. CONCLUSIONS

The area-specific resistance of $(La_{0.6}Sr_{0.4})_{0.995}Co_{0.2}Fe_{0.8}O_{3-\delta}$ (LSCF) cathode material for YSZ-based SOFCs with and without a CGO-buffer layer was measured in a symmetric cell configuration. A CGO-buffer layer between the pure LSCF

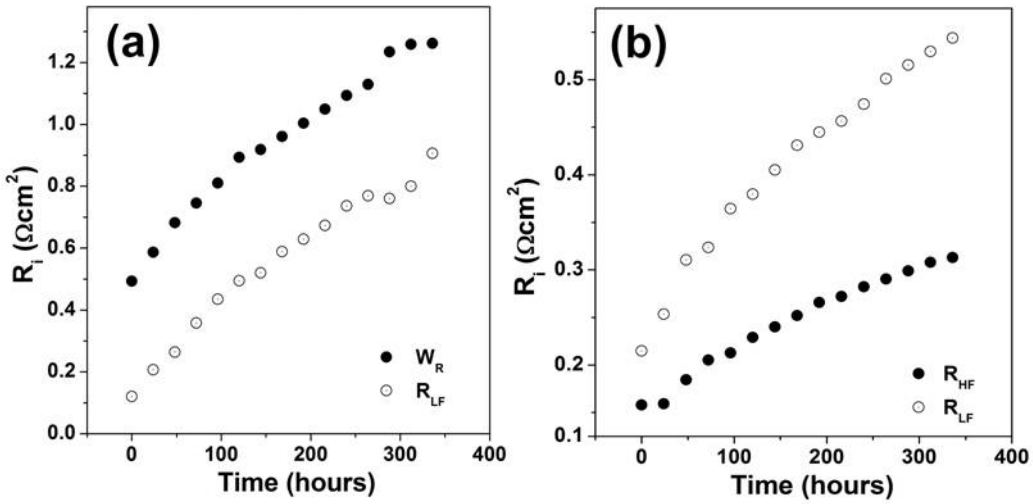

Fig. 10. Resistance (of high and low frequency processes) change as a function of time at 700ºC for LSCF/YSZ (a) and LSCF/CGO/YSZ (b) systems.

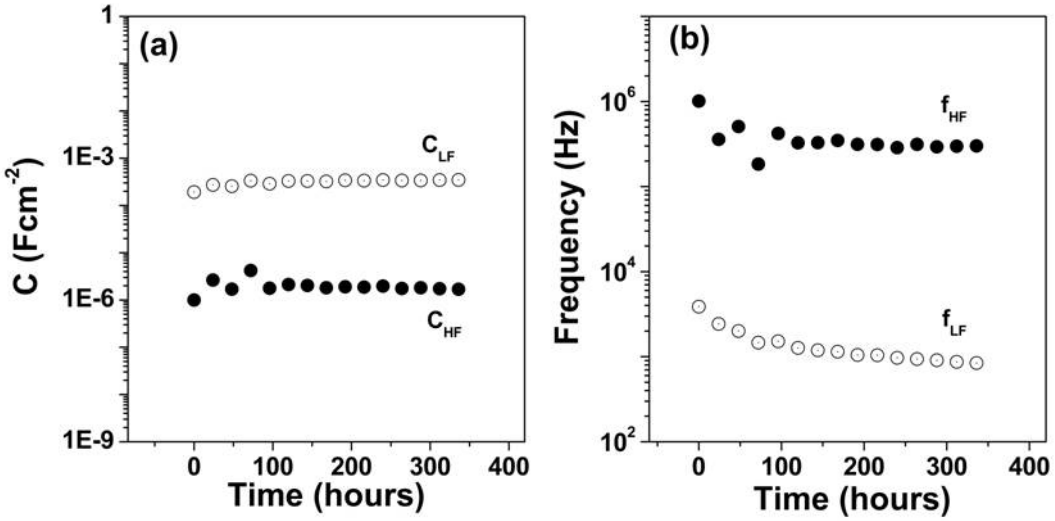

Fig. 11. Capacitance and relaxation frequency variations as a function of time at 700ºC for the LSCF/CGO/YSZ system.

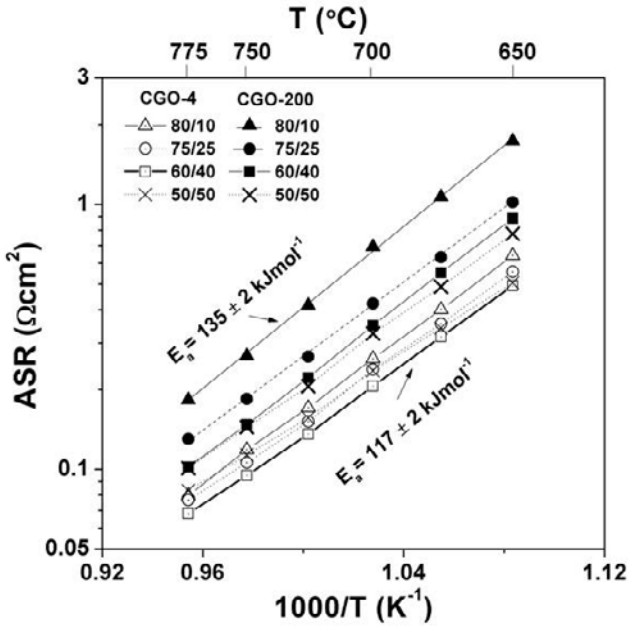

Fig. 12. Arrhenius plot of the area-specific resistance measured at different temperatures of the LSCF-CGO/CGO/YSZ systems using CGO of low and high surface area i.e. CGO-4 (4 m^2g^{-1}) and CGO-200 (200 m^2g^{-1}) for the composite preparation. The CGO-buffer layer was comprised of CGO-4 for all the systems.

cathode and the YSZ electrolyte improves the performance of the electrode. However, the polarisation resistance of pure LSCF for the symmetrical cell with the CGO-buffer layer increased from 0.325 Ωcm^2 up to 0.86 Ωcm^2 after 360 h of operation at 700ºC. Otherwise, without a CGO-buffer layer the polarisation resistance in the same ageing-test conditions increase from 0.5 Ωcm^2 to 2 Ωcm^2. Furthermore, in order to diminish the polarisation resistance of the LSCF cathode material, the addition of an ionic conducting phase, CGO in the present case, to give rise to a LSCF-CGO composite cathode material, for YSZ-based SOFC with a CGO-buffer layer, was also investigated, and polarisation resistance values as low as 0.2 Ωcm^2 at 700ºC in air were achieved for the LSFC-CGO composite with 40 wt.% of CGO.

ACKNOWLEDGEMENTS

The authors acknowledge financial support from Spanish Government (MAT2007-64486-C07-07, MAT2007-60127 and TEC2007-60996 projects and "Juan de la Cierva" and "Ramón y Cajal" fellowships for J.P-M, J.C. R-M and J. C-V.)

REFERENCES

1. S.C. Singhal, Advances in solid oxide fuel cell technology, Solid State Ionics, 135, 305-313 (2000).
2. B.C.H. Steele, A. Heinzel, Materials for fuel-cell technologies, Nature, 414, 345-352 (2001).
3. L.C. De Jonghe, C.P. Jacobson, S. J. Visco, Supported electrolyte thin film synthesis of Solid Oxide Fuel Cells, Annu. Rev. Mater. Res., 33, 169–82, (2003).
4. E. Ivers-Tiffée, A. Weber, D. Herbstritt, Materials and technologies for SOFC-components, J. Eur. Ceram. Soc., 21, 1805-1811, (2001).
5. N. P. Brandon, S.J. Skinner, B.C.H. Steele, Recent Advances in Materials for Fuel Cells, Ann. Rev. Mat. Res., 33, 183-213 (2003).
6. J.M Ralph, C. Rossignol, R. Kumar, Cathode materials for reduced-temperature SOFCs, J. Electrochem. Soc., 150, A1518-A1522 (2003).
7. A. Esquirol, J. Kilner, N. Brandon, Oxygen transport in $La_{0.6}Sr_{0.4}Co_{0.2}Fe_{0.8}O_{3-\delta}$/$Ce_{0.8}Gd_{0.2}O_{2-x}$ composite cathode for IT-SOFCs, Solid State Ionics, 175, 63-67 (2004).
8. W.G. Wang, M. Mogensen, High-performance lanthanum-ferrite-based cathode for SOFC, Solid State Ionics, 176, 457-462 (2005).
9. S. Bebelis, N. Kotsionopoulos, A. Mai, D. Rutenbeck, F. Tietz, Electrochemical characterisation of mixed conducting and composite SOFC cathodes, Solid State Ionics, 177, 1843-1848 (2006).
10. C. Fu, K. Sun, N. Zhang, X. Chen, D. Zhou, Electrochemical characteristics of LSCF-SDC composite cathode for intermediate temperature SOFC, Electrochim. Acta, 52, 4589-4594 (2007).
11. J. Chen, F. Liang, L. Liu, S. Jiang, B. Chi, J. Pu, J. Li, Nano-structured (La,Sr)(Co,Fe)O_3 + YSZ composite cathodes for intermediate temperature solid oxide fuel cells, J. Power Sources, 183, 586-589 (2008).
12. P. Ried, P. Holtappels, A. Wicher, A. Ulrich, T. Graule, Synthesis and Characterisation of $La_{0.6}Sr_{0.4}Co_{0.2}Fe_{0.8}O_3$ and $Ba_{0.5}Sr_{0.5}Co_{0.8}Fe_{0.2}O_{3-\delta}$, J. Electrochem. Soc., 155, B1029-B1035 (2008).
13. N. Grunbaum, L. Dessemond, J. Fouletier, F. Prado, L. Mogni, A. Caneiro, Rate limiting steps of the porous $La_{0.6}Sr_{0.4}Co_{0.8}Fe_{0.2}O_{3-\delta}$ electrode material, Solid State Ionics, 180 (28-31), 1448-1452 (2009).
14. H. Xiong, B.-K. Lai, A. C. Johnson, S. Ramanathan, Low-temperature electrochemical characterization of dense ultra-thin lanthanum strontium cobalt ferrite ($La_{0.6}Sr_{0.4}Co_{0.8}Fe_{0.2}O_3$) cathodes synthesized by RF-sputtering on nanoporous alumina-supported Y-doped zirconia membranes, J.Power Sources, 193, 589-592 (2009).
15. M.J. Santillán, A. Caneiro, N. Quaranta, A.R. Boccaccini, Electrophoretic deposition of $La_{0.6}Sr_{0.4}Co_{0.8}Fe_{0.2}O_{3-\delta}$ cathodes on $Ce_{0.9}Gd_{0.1}O_{1.95}$ substrates for intermediate temperature solid oxide fuel cell (IT-SOFC), Journal of the European Ceramic Society, 29, 1125-1132 (2009).
16. L.-W. Tai, M.M. Nasrallah, H.U. Anderson, D.M. Sparlin, S.R. Sehlin, Structure and electrical properties of $La_{1-x}Sr_xCo_{1-y}Fe_yO_3$. Part 1. The system $La_{0.8}Sr_{0.2}Co_{1-y}Fe_yO_3$, Solid State Ionics, 76, 259-271 (1995).
17. L.-W. Tai, M.M. Nasrallah, H.U. Anderson, D.M. Sparlin, S.R. Sehlin, Structure and electrical properties of $La_{1-x}Sr_xCo_{1-y}Fe_yO_3$. Part 2. The system $La_{1-x}Sr_xCo_{0.2}Fe_{0.8}O_3$, Solid State Ionics, 76, 273-283 (1995).
18. J.C. Ruiz-Morales, J. Canales-Vázquez, J. Peña-Martínez, D. Marrero-López, P. Núñez, On the simultaneous use of $La_{0.75}Sr_{0.25}Cr_{0.5}Mn_{0.5}O_{3-\delta}$ as both anode and cathode material with improved microstructure in solid oxide fuel cells, Electrochim. Acta 52, 278–284, (2006).
19. J. Peña-Martínez, A. Tarancón, D. Marrero-López, J.C. Ruiz-Morales, P. Núñez, Evaluation of $GdBaCo_2O_{5+\delta}$ as Cathode Material for Doped Lanthanum Gallate Electrolyte IT-SOFCs, Fuel Cells, 5, 351-350 (2008).
20. J. Peña-Martínez, D. Marrero-López, J.C. Ruiz-Morales, P. Núñez, C. Sánchez-Bautista, A.J. Dos Santos-García, J. Canales-Vázquez, On $Ba_{0.5}Sr_{0.5}Co_{1-y}Fe_yO_{3-\delta}$ (y=0.1–0.9) oxides as cathode materials for $La_{0.9}Sr_{0.1}Ga_{0.8}Mg_{0.2}O_{2.85}$ based IT-SOFCs, Int. J. Hydrogen Energy, 34, 9486-9495 (2009).
21. J. Rodríguez-Carvajal, T. Roisnel, FullProf.98 and WinPLOTR: New Windows 95/NT Applications for Diffraction Commission For Powder Diffraction, International Union for Crystallography, Newletter N°20, 1998.
22. X'Pert HighScore Plus version 2.0a, PANalytical BV 2004.
23. Inorganic Crystal Structure Database (ICSD) v2008-01.
24. A. Mineshige, J. Izutsu, M. Nakamara, K. Nigaki, J. Abe, M. Kobune, S. Fujii, T. Yazawa, Introduction of A-site deficiency into $La_{0.6}Sr_{0.4}Co_{0.2}Fe_{0.8}O_{3-\delta}$ and its effect on structure and conductivity, Solid State Ionics, 176, 1145-1149 (2005).
25. K. Świerczek, M. Gozu, Structural and electrical properties of selected $La_{1-x}Sr_xCo_{0.2}Fe_{0.8}O_3$ and $La_{0.6}Sr_{0.4}Co_{0.2}Fe_{0.6}Ni_{0.2}O_3$ perovskite type oxides, J. Power Sources, 173, 695-699 (2007).
26. G.Ch. Kostogloudis, Ch. Ftikos, Properties of A-site-deficient $La_{0.6}Sr_{0.4}Co_{0.2}Fe_{0.8}O_{3-\delta}$-based perovskite oxides, Solid State Ionics, 126, 143-151 (1999).
27. Z. Duan, M. Yang, A. Yan, Z. Hou, Y. Dong, Y. Chong, M. Cheng, W. Yang, $Ba_{0.5}Sr_{0.5}Co_{0.8}Fe_{0.2}O_{3-\delta}$ as a cathode for IT-SOFCs with a GDC interlayer, J. Power Sources, 160, 57-64 (2006).
28. Johnson D. ZView: A software Program for IES Analysis,Version 2.9c, Scribner Associates, Inc., 2005.
29. M.J. Escudero, A. Aguadero, J.A. Alonso, L. Daza, A kinetic study of oxygen reduction reaction on La_2NiO_4 cathodes by means of impedance spectroscopy, J. Electroanal. Chem., 611, 107-116 (2007).
30. H. Yokokawa, N. Sakai, T. Horita, K. Yamaji, M.E. Brito, H. Kishimoto, Thermodynamic and kinetic considerations on degradations in solid oxide fuel cell cathodes, J. Alloys and Comp., 452, 41-47 (2008).

Recibido: 30-6-09
Aceptado: 30-11-09